Heterogeneous Catalysis Hot Paper

How to cite: *Angew. Chem. Int. Ed.* **2021**, *60*, 16349–16354
International Edition: doi.org/10.1002/anie.202103960
German Edition: doi.org/10.1002/ange.202103960

Understanding Ligand-Directed Heterogeneous Catalysis: When the Dynamically Changing Nature of the Ligand Layer Controls the Hydrogenation Selectivity

*Carsten Schröder, Marvin C. Schmidt, Philipp A. Haugg, Ann-Katrin Baumann, Jan Smyczek, and Swetlana Schauermann**

Abstract: *We present a mechanistic study on the formation and dynamic changes of a ligand-based heterogeneous Pd catalyst for chemoselective hydrogenation of α,β-unsaturated aldehyde acrolein. Deposition of allyl cyanide as a precursor of a ligand layer renders Pd highly active and close to 100% selective toward propenol formation by promoting acrolein adsorption in a desired configuration via the C=O end. Employing a combination of real-space microscopic and in-operando spectroscopic surface-sensitive techniques, we show that an ordered active ligand layer is formed under operational conditions, consisting of stable N-butylimine species. In a competing process, unstable amine species evolve on the surface, which desorb in the course of the reaction. Obtained atomistic-level insights into the formation and dynamic evolution of the active ligand layer under operational conditions provide important input required for controlling chemoselectivity by purposeful surface functionalization.*

One of the major challenges in heterogeneous catalysis is a precise control over the selectivity of a catalytic process, which depends on subtle differences in the energy barriers of competing reaction pathways. A promising strategy to tackle this problem is to introduce a specific selective interaction between a reactant and an active site, which governs the chemical transformations in the desired direction. This idea has been successfully realized in enantioselective heterogeneous catalysis via functionalization of metal surfaces with ligand-like adsorbates—chiral modifiers—with many of these systems being nowadays well-understood at the mechanistic level.[1] Recently, a new type of ligand-directed heterogeneous catalysis—chemoselective catalysis—gained more attention as new highly chemoselective powdered catalysts were developed for partial hydrogenation of multi-unsaturated oxygenates or semi-hydrogenation of alkynes.[2] These developments demonstrate a great potential of this emerging technology to controllably tune the surface structure and the lateral reactant-ligand interactions in order to provide the tailor-made environment for the desired reaction steps.

Despite the impressive progress in this field demonstrated on powdered materials, the mechanistic details of the underlying ligand-directed surface processes remain only poorly understood for the most systems. Recently, we reported a mechanistic study on selective hydrogenation of an α,β-unsaturated aldehyde acrolein over Pd(111), in which the C=O bond was hydrogenated with 100% selectivity to produce the target product propenol.[3] This chemistry occurs, however, not on pristine Pd(111), but on the surface densely packed with oxopropyl ligands, which are spontaneously formed on the early stages of partial acrolein hydrogenation. Although this mechanistic study provided some starting ideas about the microscopic origin of the ligand-related effects, an in-depth atomistic understanding of the active ligand layer is largely missing. Specifically, the elementary steps leading to formation of an active ligand layer, its chemical composition and the possible dynamic changes under the reaction conditions needs to be understood, in order to approach rational design of this new promising class of materials with tailor-made catalytic properties.

Here, we report the proof-of-principal mechanistic study on purposeful formation of a catalytically highly efficient ligand layer based on model Pd(111) catalyst functionalized with allyl cyanide (AC) for selective hydrogenation of acrolein. By combination of *in operando* infrared reflection absorption spectroscopy (IRAS), scanning tunnelling microscopy (STM) and molecular beam techniques, formation and dynamic changes of the ligand layer under reaction conditions were investigated at the atomistic level. While AC forms a self-assembled 2D layer under non-reactive conditions, in which the flat lying molecules largely preserve their chemical nature, strong changes occur under the reactive conditions both in terms of the chemical nature and the spatial distribution of the ligand species. Specifically, AC transforms to N-butylimine species resulting from partial hydrogenation of the original ligand, which are adsorbed in a more upright configuration and form a more densely packed layer, adopting the hexagonal symmetry of the underlying metal. On this active layer, acrolein nearly instantaneously forms the desired propenoxy reaction intermediate followed by evolution of the target product propenol. The dynamic changes of the ligand layer induced by the reaction conditions were identified as

[*] C. Schröder, M. C. Schmidt, P. A. Haugg, A.-K. Baumann, J. Smyczek, Prof. Dr. S. Schauermann
Institute of Physical Chemistry, Christian-Albrechts-University Kiel
Max-Eyth-Str. 2, 24118 Kiel (Germany)
E-mail: schauermann@pctc.uni-kiel.de

Supporting information and the ORCID identification number(s) for the author(s) of this article can be found under: https://doi.org/10.1002/anie.202103960.

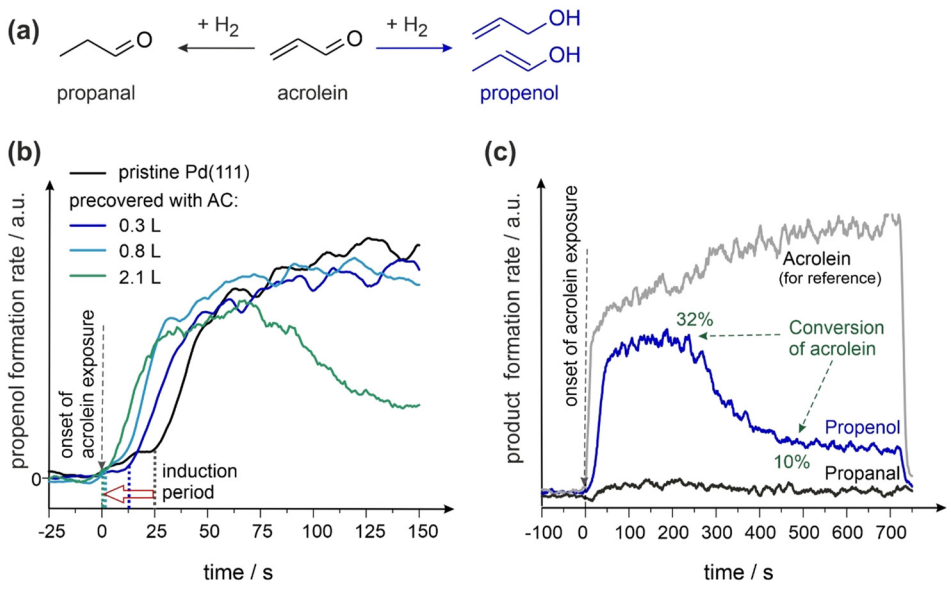

Figure 1. a) Competing reaction pathways for acrolein hydrogenation (b) Formation rates of propenol on pristine and AC-precovered Pd(111) at 250 K; c) formation rates of propenol and propanal on Pd(111) precovered with 0.8 L AC at 250 K.

a crucial process rendering the surface highly active and selective in partial hydrogenation of acrolein at the C=O bond. Obtained insights provide a deep atomistic level understanding of the most important working principles of ligand-directed heterogeneous catalysis.

Selective partial hydrogenation of acrolein, leading to formation of propenol as a target and propanal as a non-desired product (Figure 1 a), was investigated on Pd(111) surface functionalized with AC. The catalytic activity was probed by molecular beams combined with quadrupole mass spectrometry (QMS) under isothermal conditions in an apparatus described elsewhere.[4] Figure 1 b shows the time evolution of the propenol formation rate in the gas phase for pristine and AC-precovered Pd(111) at different AC coverages. In each experiment, the surface was first exposed continuously to a H_2 beam, at a time indicated as zero the second molecular beam was opened to dose acrolein (for details see Supporting Information, SI; in the following, the simultaneous exposure to H_2 and acrolein at the reaction temperature will be denoted as "reaction conditions" for the reactivity measurements). On pristine Pd(111), a prolonged induction period is observed before the onset of propenol evolution. Previously, we have shown that during the induction period an oxopropyl ligand layer is formed as a result of a single H insertion into the C=C bond of adsorbed acrolein, which turns the surface close to 100 % selective toward C=O bond hydrogenation.[3,5] On Pd(111) functionalized with AC prior the reaction, the induction period becomes either strongly reduced at intermediate AC coverages or even completely vanishes at coverages close to a monolayer. For all functionalized surfaces propenol is formed with the estimated selectivity in the range 95–100 %, which will be denoted in the following as "close to 100 %", and fairly high conversion (up to 32 %) as exemplarily shown in Figure 1 c. These observations demonstrate that surface functionalization with AC renders it highly selective and can be used for rational design of ligand-containing catalysts without relying on spontaneous formation of the oxopropyl ligand layer.

To get more insights into the formation of the active ligand layer and the reaction intermediate, a combination of *in operando* IRAS and kinetic studies via molecular beams was performed in a broad reaction parameter range. Figure 2 a shows the propenol formation rate over AC-functionalized Pd(111) at 250 K upon pulsing of acrolein onto the surface continuously exposed to H_2. During the indicated periods of time (1–5), IR spectra were obtained on this surface, shown in Figure 2 b as spectra 1–5. The spectrum 0 corresponds to the same surface prior to exposure to acrolein. On this non-reactive surface, two most important peaks are observed at 1746 and 1582 cm^{-1}, which are not present in non-perturbed AC and are related to a partly hydrogenated derivatives of AC. The band at 1746 cm^{-1} was previously described as a (C=N···Pd) stretching vibration for structurally similar acetonitrile and methyl isocyanide.[6] The band at 1582 cm^{-1} is typical of $\delta(NH_2)$ deformation vibration in simple amines.[7] While the exact nature and formation of these species will be discussed the detail later, it is important to point out that AC does not retain its original chemical structure in presence of H_2 and transforms to two new species with spectroscopic signatures characteristic of imines and amines. Upon dosing of acrolein (spectra 1–4), a new band at 1166 cm^{-1} appears nearly instantaneously on AC-functionalized Pd(111), which presence strongly correlates with the evolution of propenol in the gas phase, and vanishes when the acrolein beam is interrupted (spectrum 5). Following the assignment made in our previous study on pristine Pd(111), we attribute this band to a C-O vibration in a direct reaction intermediate (RI) propenoxy-species CH_2=CH–CH–O···Pd, in which the C-O entity is attached to Pd through the O atom (for details see SI, Chapter IV). Importantly, on the AC-covered surface, this band shifts by 46 cm^{-1} pointing to a strong lateral interaction between the RI and the ligand layer.

Another striking observation is that the evolution of two prominent AC-related surface species is not directly correlated with the reactant supply or evolution of the target product propenol: the imine species containing a C=N···Pd bond (1746–1755 cm^{-1}) remain constantly present on the surface irrespectively of the reactant supply, while the species containing a -NH_2 group slowly disappear in the course of the reaction. Additionally, a band at 1330 cm^{-1} evolves, which results from partial decomposition of acrolein to ethylidyne-

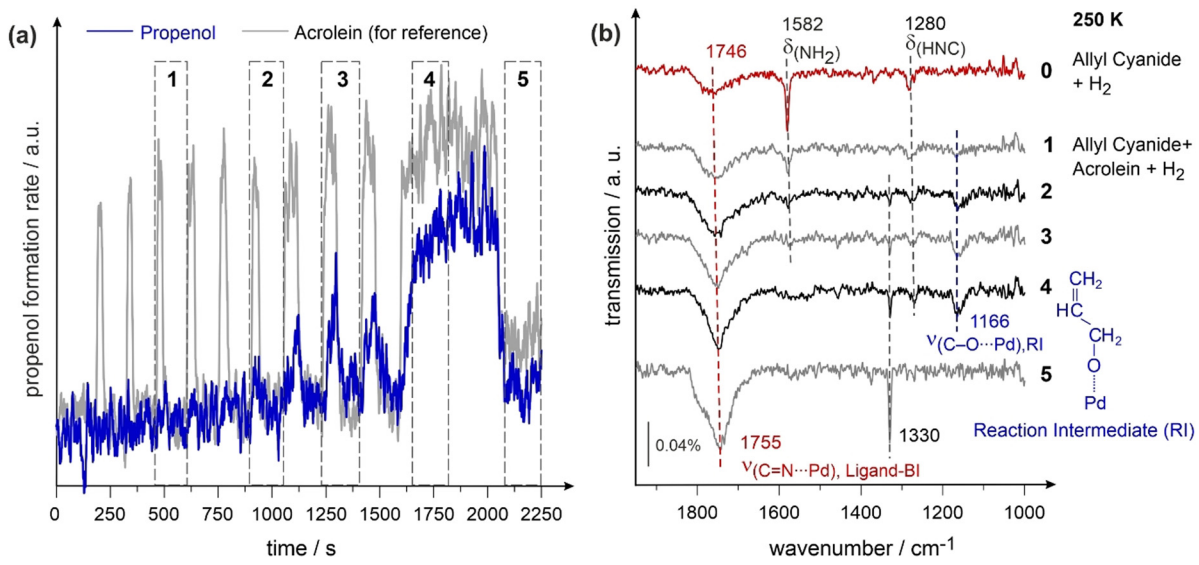

Figure 2. a) Formation rate of propenol on Pd(111) precovered with 1.0 L AC at 250 K measured in a pulsed experiment; b) IR spectra of 1.0 L AC prior the beginning of the reaction (spectrum 0) and IR spectra obtained on the same surface after the beginning of the reaction. The spectra 1–5 were obtained during the time slots indicated in (a) as 1–5; full details can be found in Chapter II in SI.

like species.[8] The evolution of these species is responsible for reactivity decrease after the initial period of high propenol formation rate (more details on reactivity decrease in Chapter VIII in SI).

These datasets provide a clear indication that formation of the direct RI propenoxy (CH_2=CH−CH−O···Pd) species and the target product propenol is strongly affected by the ligand formed under the reaction conditions on the AC-functionalized surface.

To get more atomistic level insights into the chemical and geometric structure of the active ligand layer forming and dynamically changing under the reaction conditions, a combined microscopic and spectroscopic study was performed on AC adsorbed on pristine and H-containing Pd(111) in a broad temperature range. Figure 3 shows the STM images obtained under non-reactive (Figure 3a–c) vs. reactive conditions (Figure 3d). Note that the term "reaction conditions" for STM measurements is related to AC adsorbed on Pd(111) in presence of H_2 at the specific reaction temperature. In both cases, AC adsorbates form ordered layers on these surfaces, exhibiting, however, strongly different patterns. To the best of our knowledge, this is the first experimental proof of the formation of an active ligand layer obtained by real space microscopy (Figure 3d), which exhibits a high degree of ordering and by this provides a specific confinement, allowing for a desired adsorption configuration of the reactant. In our previous studies on acrolein hydrogenation, formation of an ordered oxopropyl ligand layer was hypothesized,[3a] but was not yet proven experimentally. Complementarily, the chemical nature of the adsorbed species was investigated by IRAS on both types of surfaces (Figure 4).

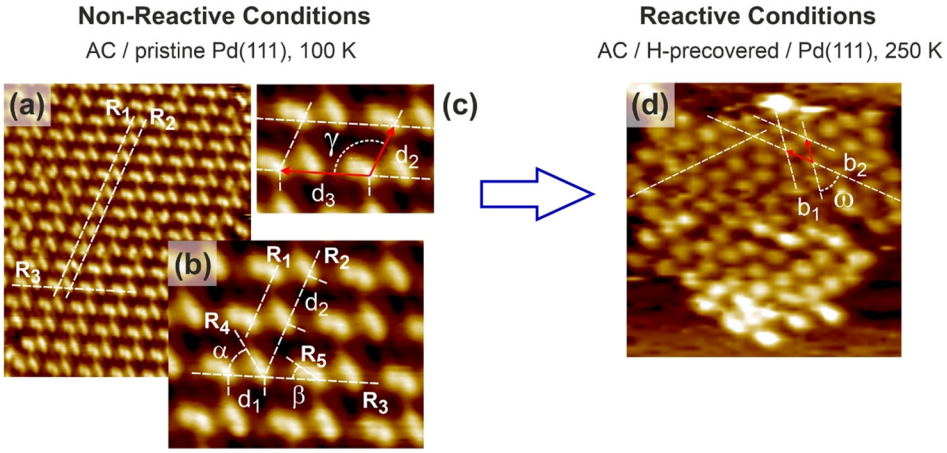

Figure 3. a) STM image of allyl cyanide on pristine Pd(111) at 230 K (15.9×19.1 nm^2); b) close-up image (5.8×4.6 nm^2) from (a) indicating three main rows in the 2D self-organized AC layer; c) close-up image showing the unit cell of the 2D AC layer; d) STM image of allyl cyanide on H-precovered Pd(111) at 250 K (10.6×10.8 nm^2). Full experimental details can be found in Chapter II in SI.

Under non-reactive conditions, AC forms a 2D self-assembled layer (Figure 3a–c), which consists of individual entities, each showing a brighter (head) and darker (tail) protrusions. Generally, each adsorbate in this layer exhibits a 2-point interaction, which is realized via interaction of each head with two tails and each tail with two heads. Figure 3b shows this structure in more detail: there are two parallel rows R_1 and R_2 of adsorbates, which are inclined with respect to the axis R_3 by $69 \pm 1°$. The distance between the heads in the row R_3 $d_1 = 8.3 \pm 0.2$ Å,

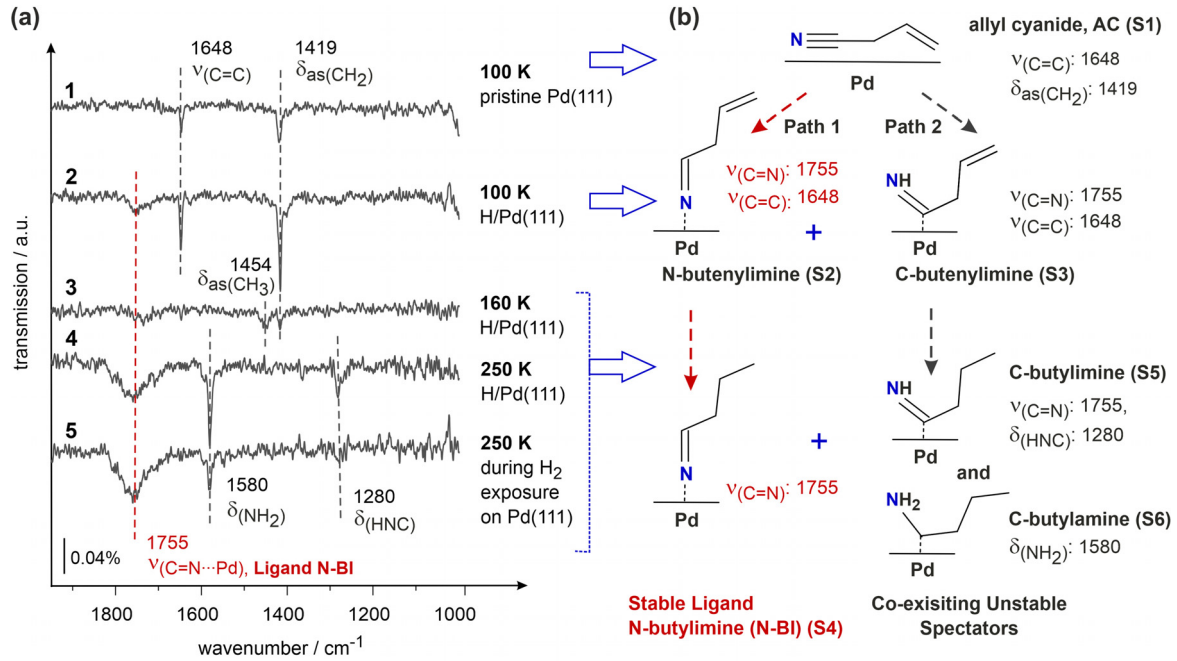

Figure 4. a) IR spectra of AC adsorbed on Pd(111) at indicated temperatures. The spectrum 1 is obtained on pristine and the spectra 2–4 on H-precovered Pd(111). Spectrum 5 is recorded during continuous H_2 exposure under the reaction conditions (full details can be found in Chapter II in SI); b) Reaction Scheme showing chemical transformations of AC according to two competing reaction pathways as deduced from (a).

which corresponds to $(3.0 \pm 0.1) \times d_{\text{Pd-Pd}}$ with $d_{\text{Pd-Pd}}$ being the spacing between two Pd atoms (2.75 Å). The distance d_2 between two heads along the rows R_1 and R_2 amounts to $(4.8 \pm 0.1) \times d_{\text{Pd-Pd}}$. The main axis R_4 of the molecules lying in the row R_1 is inclined with respect to the axis R_3 by $\alpha = 61 \pm 1°$, while the main axis R_5 of the molecules constituting the row R_2 is tilted by the angle $\beta = 37 \pm 1°$ with respect to R_3. Figure 3c shows the unit cell of the AC 2D self-organized layer with the lattice parameters $d_2 = (4.8 \pm 0.1) \times d_{\text{Pd-Pd}}$; $d_3 = (7.6 \pm 0.1) \times d_{\text{Pd-Pd}}$ and $\gamma = 106 \pm 1°$.

The IR spectra related to non-reactive conditions are shown in Figure 4a (spectrum 1, 100 K) and in Figure SI_2 in SI (100–250 K). At 100 K, only two major vibrational bands are observed: at 1648 (ν(C=C)) and 1419 cm^{-1} (δ(CH_2)), while the normally intense band related to the CN-group (2250 cm^{-1}) is not seen.[9] The latter observation originates most likely from the nearly parallel orientation of the CN-group with respect to the metal plane making it invisible for IRAS due the metal surface selection rule (MSSR).[10] At elevated temperatures, the intensity of both bands (1648 and 1419 cm^{-1}) strongly decrease most probably due to the changes in the adsorption configuration making the entire molecule oriented nearly flat with respect to the metal plane (for additional discussion see SI, Chapter V), which is consistent with the elongated form of the adsorbates imaged by STM. Combined microscopic and spectroscopic information result in the atomistic model of this ligand layer under non-reactive conditions shown in Figure 5a. The adsorbates are separated by $5 \times d_{\text{Pd-Pd}}$ along the row R_3, while the distance between R_1 and R_2 corresponds to the separation by $3 \times d_{\text{Pd-Pd}}$. The angles between the molecular axes with respect to R_3 (α and β) amount to ≈37° and 61°, respectively. The mutual intermolecular interactions between the adsorbates are most likely based on H-bonding between the N-atom of each molecule and the H atoms of the terminal CH_2 group of two neighboring adsorbates (visualized by red dotted lines). It should be noted that while the exact position of the CN groups cannot be derived unambiguously from the STM data, it is likely that the electron rich CN group is related to the brighter part of the molecule, that is, the head-position.

Upon transition to the reactive conditions, the 2D self-assembled ligand layer undergoes dramatic changes both in terms of the geometric structure and the chemical nature of the adsorbates. Here, an ordered layer of the hexagonal symmetry is formed (Figure 3d) with the adsorbates exhibiting a nearly round footprint in STM. The spacing between the adsorbates along the axes shown in Figure 3d is $b_1 = (2.7 \pm 0.3) \times d_{\text{Pd-Pd}}$ and $b_2 = (3.1 \pm 0.1) \times d_{\text{Pd-Pd}}$ (red vectors b_1 and b_2 show the unit cell of this layer; $\omega = 53 \pm 2°$). This transition is also accompanied by substantial changes in the chemical composition of the originally deposited AC ligand. Figure 4a shows the IR spectra obtained on H-precovered Pd(111) surface at successively increasing temperatures (spectra 2 and 3), which finally reaches the state of the catalyst under operational conditions (spectra 4 and 5). At 100 K, AC adsorbed on H-covered surface still retains two peaks typical of molecularly adsorbed AC: 1648 (ν(C=C)) and 1419 (δ-(CH_2)) cm^{-1}.[9] Importantly, a new peak at 1755 cm^{-1} appears, which is present neither in multilayer nor in the gas phase AC.[9] Previously, this vibration was observed for structurally similar molecules acetonitrile and methyl isocyanide upon adsorption on Pd(111)[6b] and was attributed to imine species, in which the band at 1755 cm^{-1} is related to the stretching vibration of the (C=N) bond in the (-C=N···Pd) fragment. This

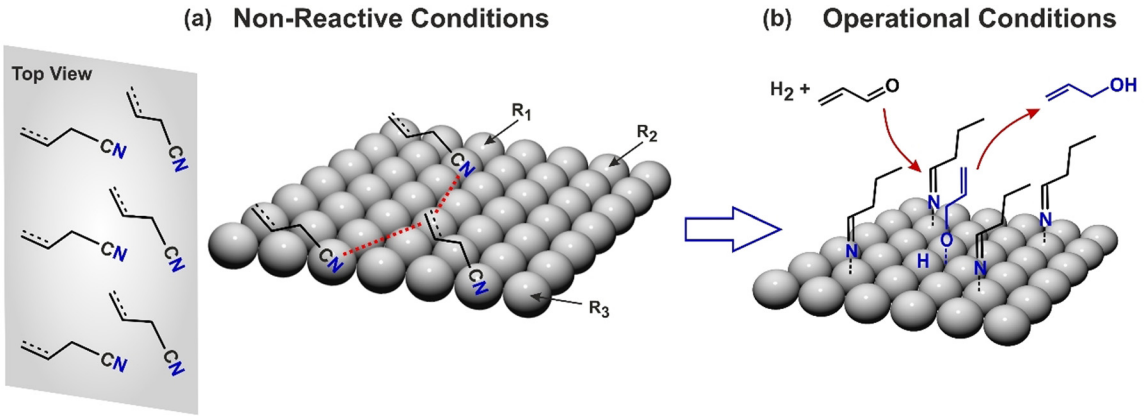

Figure 5. Model of adsorbed AC-derived species under a) non-reactive and b) operational conditions in presence of H_2 and acrolein. For additional discussion on the AC structure in (a), see SI, Chapter V.

observation suggests partial reduction of the C≡N triple to the C=N double bond accompanied by formation of the species strongly bound to Pd. Generally, two possible configurations of these species are possible: bound either through the N or the C atom, which are shown in the scheme of the Figure 4b and indicated as N- and C-butenylimine (S2 and S3, respectively).

At 160 K, the further hydrogenation step occurs giving rise to *(i)* disappearance of the peaks at 1648 (ν(C=C)) and 1419 ($\delta(CH_2)$) cm^{-1} and *(ii)* appearance of a new peak at 1454 cm^{-1} corresponding to the CH_3 deformation vibration ($\delta(CH_3)$).[11] The combination of these observations suggest that the C=C bond becomes hydrogenated in this temperature range and a new terminal -CH_3 group appears.

At 250 K (spectra 4 and 5), further hydrogenation steps occur mainly resulting in *(i)* significant growth of the peak at 1755 cm^{-1} (-C=N···Pd) and *(ii)* appearance of two new peaks at 1580 and 1280 cm^{-1}, which are characteristic of -NH_2 and HNC deformation vibrations, respectively.[12] Simultaneous appearance of these bands means that both imine and amine species are formed and co-exist in this temperature range. It also suggests that at least two reaction pathways run in parallel to transfer the originally deposited AC to co-existing imine and amine surface species.

Figure 4b displays a model for the proposed AC reaction pathways, which is consistent with all spectroscopic observations. For all species, the characteristic bands employed for assignment are given next to the proposed structure. At 100 K, AC deposited on pristine Pd(111) exhibits an adsorption geometry with the CN group oriented nearly parallel to the surface, while the C=C group is inclined and hence visible in IRAS (species S1). When H is co-adsorbed at 100 K, a fraction of these species is capable of forming the imine group (-C=N···Pd, 1755 cm^{-1}). The formed butenylimine species can be bound to the surface either via the N-end (N-butenylimine, S2 species) or via the C-atom (C-butenylimine, S3 species) and undergo further partial hydrogenation steps. In the first pathway, the N-butenylimine species (S2) is hydrogenated at the C=C bond producing the N-butylimine (S4) species in the temperature range 160–250 K. In the second pathway, the C-butenylimine (S3) species are also hydrogenated at the C=C bond forming C-butylimine species (S5). However, hydrogenation does not stop at this stage and in the fraction of S5 species, the imine group is hydrogenated to amine forming C-butylamine species (S6). The species S5 and S6 co-exist on the surface and evolve in a very similar way: they appear in the same temperature range and both disappear in a correlated way upon prolonged H_2 exposure in the course of the reaction as can be deduced from the comparison of the spectra 4 and 5 in Figure 4b. Note that the characteristic vibrations used to identify the species S5 and S6 (δ(HNC) at 1280 and $\delta(NH_2)$ at 1580 cm^{-1}) cannot originate from the same surface species. On the other hand, the nearly identical evolution of these species upon temperature variation and prolonged exposure to H_2 suggest that the species S5 and S6 are strongly correlated, most likely as a precursor (S5) and the product (S6). Thus, the combination of all spectroscopic data suggest that the originally adsorbed AC species S1 becomes partly hydrogenated under the reaction conditions along two competing reaction pathways: the first one leads to formation of the N-butylimine (S4) species, while the second results in the formation of the mixture of C-butylimine (S5) and C-butylamine (S6) species.

It is important to emphasize that one type of species—N-butylimine (S4)—remains present on the catalytic surface under the reaction conditions and serves as an active ligand layer. The other two species—C-butylimine (S5) and C-butylamine (S6)—quickly disappear after prolonged H_2 exposure (see Figure 4b, spectra 4 and 5; Figure 2, spectra 0–5), most likely as a result of successive hydrogenation of the C=N bond of C-butylimine (S5) to C-butylamine (S6) followed by H insertion into the C···Pd bond to produce molecular butylamine that is able to desorb (for additional discussion on the stability of S5 and S6 species see SI, Chapter X; the stability of the S4 species is additionally discussed in SI, Chapter III). This observation suggests that species building an active ligand layer under the reaction conditions are the stable N-butylimine (S4) species, while the mixture of the unstable species C-butylimine (S5) and C-butylamine (S6) are the spectators disappearing in the course of the reaction without effecting the catalytic efficiency.

Figure 5b shows the model of the geometric orientation of the active N-butylimine (S4) species based on the STM data: all ligand molecules are separated by approx. $3 \times d_{\text{Pd-Pd}}$, meaning that each third Pd atom along the main axis is covered by the ligand. The clearly visible band at 1755 cm^{-1} characteristic of the imine species suggests a rather upright adsorption geometry, which is also reflected in this model.

Summarizing, we provide for the first time a comprehensive atomistic level description of a ligand-based heterogeneous catalyst for chemoselective hydrogenation of α,β-unsaturated aldehyde acrolein. Deposition of allyl cyanide as a precursor of an active ligand layer renders the catalyst highly active and close to 100% selective toward propenol formation and eliminates the induction period observed on pristine surfaces. Formation and dynamic evolution of the active ligand layer under the reaction conditions were investigated by combination of *in operando* spectroscopic and microscopic surface sensitive techniques. On pristine Pd and under non-reactive conditions, AC forms a self-assembled 2D layer with the species oriented close to parallel to the surface and exhibiting a two-point interaction between the -CN and the CH_x groups of neighboring molecules. Upon transferring to the reaction conditions, both the chemical nature of the adsorbates and the geometric configuration of the ligand layer drastically change. In two competing reaction pathway, both stable N-butylimine active ligand species and unstable spectator species are formed. These latter species comprising C-butylamine and C-butylimine desorb in the course of the reaction after prolonged H_2 exposure. The stable N-butylimine species forms an ordered ligand layer acting under the reaction conditions, in which every third Pd atom is covered by N-butylimine adsorbate. With this we provide for the first time a direct microscopic proof that ordered layers of active ligand species are formed, which govern the interaction of acrolein with the catalyst by lateral interactions and by this render the surface highly chemoselective.

Obtained atomistic-level insights highlight the exceptional importance of controlling the chemical and geometrical structure of dynamically changing active ligand layer under operational conditions. Related effects are expected to play a key role for chemoselective hydrogenation of all types of multi-unsaturated hydrocarbons over ligand-functionalized catalysts including practically relevant powdered materials.

Acknowledgements

This work has been supported by the German Science Foundation (DFG, Grant SCHA 1477/6-1). Open access funding enabled and organized by Projekt DEAL.

Conflict of interest

The authors declare no conflict of interest.

Keywords: chemoselective hydrogenation · functionalized surfaces · heterogeneous catalysis · infrared spectroscopy · scanning tunnelling microscopy

[1] a) F. Meemken, A. Baiker, *Chem. Rev.* **2017**, *117*, 11522; b) A. J. Gellman, W. T. Tysoe, F. Zaera, *Catal. Lett.* **2015**, *145*, 220.
[2] a) S. G. Kwon, et al., *Nano Lett.* **2012**, *12*, 5382; b) S. T. Marshall, J. W. Medlin, *Surf. Sci. Rep.* **2011**, *66*, 173; c) S. T. Marshall, et al., *Nat. Mater.* **2010**, *9*, 853; d) P. Sonström, M. Baumer, *Phys. Chem. Chem. Phys.* **2011**, *13*, 19270.
[3] a) K.-H. Dostert, et al., *J. Am. Chem. Soc.* **2015**, *137*, 13496; b) K.-H. Dostert, et al., *ACS Catal.* **2017**, *7*, 5523; c) S. Schauermann, *J. Phys. Chem. Lett.* **2018**, *9*, 5555.
[4] S. Attia, E. J. Spadafora, J. Hartmann, H.-J. Freund, S. Schauermann, *Rev. Sci. Instrum.* **2019**, *90*, 053903.
[5] C. P. O'Brien, K.-H. Dostert, S. Schauermann, H.-J. Freund, *Chem. Eur. J.* **2016**, *22*, 15856.
[6] a) S. Katano, et al., *J. Phys. Chem. B* **2006**, *110*, 20344; b) K. Murphy, S. Azad, D. W. Bennett, W. T. Tysoe, *Surf. Sci.* **2000**, *467*, 1.
[7] a) D. Jentz, H. Celio, P. Mills, M. Trenary, *Surf. Sci.* **1995**, *341*, 1; b) W. Erley, J. C. Hemminger, *Surf. Sci.* **1994**, *316*, L1025.
[8] F. Zaera, *Langmuir* **1996**, *12*, 88.
[9] J. R. Durig, G. A. Guirgis, A. S. Drew, *J. Raman Spectrosc.* **1994**, *25*, 907.
[10] F. M. Hoffmann, *Surf. Sci. Rep.* **1983**, *3*, 107.
[11] D. C. McKean, et al., *Spectrochim. Acta Part A* **1985**, *41*, 435.
[12] L. Vogt, E. Schulte, S. Collins, P. Quaino, *Top. Catal.* **2019**, *62*, 1076.

Manuscript received: March 19, 2021
Revised manuscript received: May 3, 2021
Accepted manuscript online: May 19, 2021
Version of record online: June 18, 2021

